observed. If chelate ring closure is involved in the formation of these metal–ligand complexes, then the observed rate constant results indicate that $k_0' \lesssim k_{-0}$ for the Ni(II) and Co(II) complexes, while, for the Al(III), Fe(III), and V(IV) complexation reactions, $k_0' \gg k_{-0}$.

The internal hydrogen-bond[6,7] mechanism is also applicable to the aforementioned metal ion complexation reactions. In this mechanism metal ion attack at the reactive site of the ligand is blocked by a proton hydrogen-bound to the site. An example for α-substituted carboxylic acids is

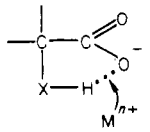

X = S, O, or NH_2
M^{n+} = metal ion
n = 2,3
··· = hydrogen bond

With such a mechanism, ligand reactivity can vary from metal ion to metal ion if the rate of substitution is dependent on the ability of the metal ion to displace the proton blocking the reactive site. Thus, the normal complexation rate constants observed for Al(III), Fe(III), and V(IV) may be due to their greater ability relative to Co(II) and Ni(II) to break hydrogen bonds.

In Table IV an increase in k_1 values for the Ni^{2+} complexation reactions is observed as the ligand substituent on the carbon adjacent to the carboxylic group is varied from NH_2 to OH to SH. This trend can be explained in terms of both the internal hydrogen bond mechanism and the SCS mechanism. In the first case the strength of the internal hydrogen bond can be assumed to decrease with the increasing acidity of the substituent group. Consequently, since the acidities of the substituents follow the order SH > OH > NH_2, Ni(II) complex formation with thiolactic acid might be expected to occur more rapidly than with vanillomandelic and mandelic acids. Similar rate increases with increasing ligand acidity are observed for the Ni(II) complexation reactions[10] with salicylic, sulfosalicylic, and anthranilic acids.

Considering the rate-determining ring closure mechanism, it is conceivable that because of its larger size the thiol group in thiolactic acid may be more favorably positioned for chelate ring closure about the nickelous ion than the corresponding hydroxyl group in vanillomandelic and mandelic acids, and even more so than the amino group in anthranilic acid. Thus, the observed order of reactivity can also be explained in terms of some subtle steric differences between the different ligands.

The complex dissociation constants (k_{-1}) given in Table III are of almost exactly the same value for all three ligands. Thus, complex stability is seen to increase with increasing ligand acidity. Though this is an unusual trend for Ni^{2+}, it has been observed for a number of Ni^{2+}–ligand complexation reactions[6] in which internal hydrogen bonding was postulated to play a part in the kinetics scheme.

Acknowledgment. The authors thank the U.S. Public Health Service for the support provided by Research Grant GM08893-16 from the National Institute of General Medical Sciences.

Registry No. Vanillomandelic acid, 55-10-7; mandelic acid, 90-64-2; thiolactic acid, 79-42-5; Ni^{2+}, 14701-22-5.

(21) Saini, G.; Mentasti, E. *Inorg. Chim. Acta* **1970**, *4*, 585.

Contribution from the Department of Chemistry, Faculty of Science, Hokkaido University, Sapporo 060, Japan

Temperature-Jump Studies of the Ligand Substitution Reactions of Tetrahedral Cobalt(II) Complexes Solubilized in Reversed Micelles

AKIHIKO YAMAGISHI,* TAKESHI MASUI, and FUMIYUKI WATANABE

Received December 5, 1979

The kinetics of ligand substitution of tetrahedral complexes of the Co(II) ion solubilized in reversed micellar systems were studied by means of a temperature-jump method. The investigated reactions are (1) $CoCl_4^{2-} + SCN^- \rightleftharpoons CoCl_3(SCN)^{2-} + Cl^-$ in dodecylpyridinium chloride (DPC)/chloroform and (2) $CoCl_3(SCN)^{2-} + SCN^- \rightleftharpoons CoCl_2(SCN)_2^{2-} + Cl^-$ in DPC/water/chloroform. In both reactions, the experimental data fit the mechanisms $CoCl_3X^{2-} \rightleftharpoons CoCl_2X^- + Cl^-$, followed by $CoCl_2X^- + SCN^- \rightleftharpoons CoCl_2X(SCN)^{2-}$, where X = Cl^- and SCN^- for reactions 1 and 2, respectively. The backward rate constants of the second step or the formation of tricoordinate intermediate from $CoCl_2X(SCN)^{2-}$ are obtained to be $(5.5 \pm 2.0) \times 10^3$ and $(3.7 \pm 1.0) \times 10^4$ s^{-1} at 20 °C for reactions 1 and 2, respectively. The present results were discussed in comparison with the reported ligand-exchange kinetics of other tetrahedral Co(II) complexes.

Although the mechanism of ligand replacement in an octahedral complex is well established,[1] relatively little is known about substitution reactions of tetrahedral complexes.[2] One of the difficulties in studying the above topic lies in the fact that many complexes which are tetrahedral in crystalline state yield six-coordinate solvated complexes in donor solvents.

Recently we have investigated the structure and reaction of metal complexes solubilized in surfactant aggregates in nonpolar medium (termed as reversed micellar systems).[3-5] It was revealed that, in the polar interior of a reversed micelle, tetrahedral complexes of the Co(II) ion are stably present even in the presence of cosolubilized water.[5,6] On the basis of this finding, we have decided to study the ligand substitution reactions of tetrahedral Co(II) complexes in the reversed micellar system. The mechanisms of ligand exchange of tetrahedral Co(II) complexes have been investigated so far only in a few examples, all of which were performed in nonpolar solvents.[7-9]

(1) R. G. Wilkins, *Acc. Chem. Res.*, **3**, 408 (1970).
(2) H. Werner, *Angew. Chem., Int. Ed. Engl.*, **7**, 930 (1968).
(3) T. Masui, F. Watanabe, and A. Yamagishi, *J. Colloid Interface Sci.*, **61**, 388 (1977).
(4) T. Masui, F. Watanabe, and A. Yamagishi, *J. Phys. Chem.*, **81**, 494 (1977).
(5) A. Yamagishi, F. Watanabe, and T. Masui, *J. Phys. Chem.*, **84**, 34 (1980).
(6) J. Sunamoto and T. Hamada, *Bull. Chem. Soc. Jpn.*, **51**, 3130 (1978).

0020-1669/81/1320-0513$01.00/0

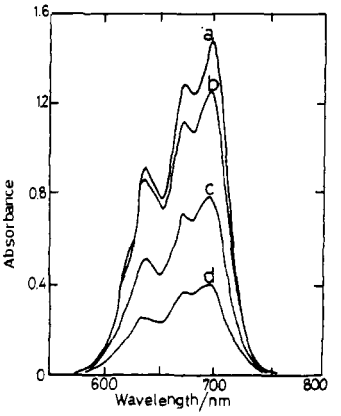

Figure 1. Electronic spectrum of $CoCl_2$ solubilized in the DPC/H_2O/$CHCl_3$ system. $[H_2O]$ = (a) 0, (b) 0.13, (c) 0.24, and (d) 0.35 M, $[CoCl_2]$ = 2.2×10^{-3} M, and [DPC] = 0.11 M.

In this paper are presented results of reactions 1 and 2, in dodecylpyridinium chloride (DPC)/chloroform and DPC/water/chloroform, respectively.

$$CoCl_4^{2-} + SCN^- \rightleftharpoons CoCl_3(SCN)^{2-} + Cl^- \quad (1)$$

$$CoCl_3(SCN)^{2-} + SCN^- \rightleftharpoons CoCl_2(SCN)_2^{2-} + Cl^- \quad (2)$$

Experimental Section

Anhydrous $CoCl_2$ and KSCN (both purchased from Wako Pure Chemical Ind.) were dried under vacuum for 2 days. Dodecylpyridinium chloride (DPC) (Kanto Kagaku Co.) was recrystallized twice from acetone. Chloroform was distilled twice over molecular sieves (water content less than 0.12 mg/mL). Deuterium oxide (99.75%) was purchased from Merck.

Electronic spectra were measured with a Hitachi EPS-3T spectrophotometer. Equilibrium constants were determined at 20 °C. Rates were measured with a Union Giken temperature-jump apparatus with a coaxial cable.[10] Concentration change resulting from temperature perturbation was followed photometrically in the range 550–700 nm. The signal was stored in a Kawasaki TM-2720DS transient memory and then displayed on a recorder. Before the discharge, a sample solution was thermostated at 17 °C. The temperature rise was estimated to be ca. 3 °C at the discharge voltage of 17.5 kV. The time course of the temperature rise was monitored, following the dimerization reactions of the sodium salt of the 2,3-dichloro-5,6-dicyano-*p*-benzoquinone anion radical, which equilibrates much faster than the temperature rise of the present apparatus.[10] The calculations for determining K_{21}, K_{31}, and K_{22} from the electronic spectra (Figure 3) were performed with an electronic computer, PANAFACOM U-400.

Results and Calculations

Equilibrium Results. Anhydrous $CoCl_2$ is insoluble in chloroform. The compound displays deep blue color, when it is solubilized in a chloroform solution of DPC (0.1–0.3 M).[5] By comparison of the absorption peaks at 696, 668, and 633 nm of the spectrum (Figure 1) with the reported data,[11] it is confirmed that Co(II) is solubilized in the DPC aggregates as a tetrahedral $CoCl_4^{2-}$ complex.[5]

Figure 2 shows the change of spectrum on adding KSCN to a solution containing constant amounts of $CoCl_2$ and DPC. A clear isosbestic point at 685 nm indicates that a conversion between two light-absorbing species occurs. If one Cl^- in $CoCl_4^{2-}$ is replaced by SCN^- (eq 1), the observed difference

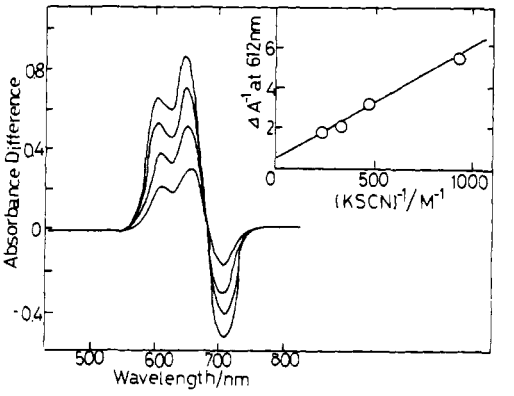

Figure 2. Difference spectra between a solution of $CoCl_2$ (0.0020 M) and DPC (0.14 M) as a reference cell and a solution of $CoCl_2$ (0.0020 M), DPC (0.14 M), and a various amount of KSCN. [KSCN] = (a) 0.003 98 M, (b) 0.003 06, (c) 0.002 09, and (d) 0.001 07 M, respectively. The inset shows a plot of the recpirocal of difference absorbance at 612 nm, ΔA^{-1}, against the recpirocal of [KSCN].

in absorbance, ΔA, is related to the concentrations of Cl^- and SCN^- as shown in eq 3, where $\Delta\epsilon$ is the difference of the molar

$$\frac{1}{\Delta A} = \frac{1}{\Delta\epsilon M_0}\left(\frac{[Cl^-]}{K_1[SCN^-]} + 1\right) \quad (3)$$

extinction coefficient between $CoCl_3(SCN)^{2-}$ and $CoCl_4^{2-}$ and M_0 is the total amount of Co(II) ion, respectively. K_1 is the apparent equilibrium constant of eq 1 expressed in terms of concentrations instead of activities. The concentrations of the reactants are expressed on the basis of the following assumptions: (i) KSCN is dissociated into free ions in the DPC aggregates; (ii) all SCN^- ions react with $CoCl_4^{2-}$ with equal reactivity; (iii) one DPC molecule provides one Cl^- ion which participates in equilibrium 1. Under the above assumptions, $[Cl^-]$ and $[SCN^-]$ are equated to [DPC] and [KSCN], respectively, where the brackets denote the analytical concentration of the species. When ΔA^{-1} at 612 nm is plotted against the reciprocal of [KSCN], a straight line is obtained as seen in the inset of Figure 2. With application of eq 3 to the plot, K_1 is determined to be 20 ± 6. In case that [DPC] is varied at the constant amount of KSCN, the similar absorption change as in Figure 2 is obtained. In this case, ΔA^{-1} increases linearly with [DPC]. From this plot, K_1 is obtained to be 17 ± 5. The agreements between these two K_1 values within the experimental error validates both relation 3 and the above assumptions.

When water is added to a solution of $CoCl_2$ and DPC, the absorbance due to $CoCl_4^{2-}$ decreases with no change of spectral shape (Figure 1). According to the previous analysis, $CoCl_4^{2-}$ is aquated by way of the two-step schemes[5] (4) and (5), with

$$CoCl_4^{2-} + 4H_2O \rightleftharpoons CoCl_2(H_2O)_4 + 2Cl^- \quad K_4 \quad (4)$$

$$CoCl_2(H_2O)_4 + 2H_2O \rightleftharpoons Co(H_2O)_6^{2+} + 2Cl^- \quad K_5 \quad (5)$$

$K_4 = [CoCl_2(H_2O)_4]_m[Cl^-]_m^2/[CoCl_4^{2-}]_m[H_2O]_m^4$ and $K_5 = [Co(H_2O)_6^{2+}]_m[Cl^-]_m^2/[CoCl_2(H_2O)_4]_m[H_2O]_m^2$. Here, the concentrations of reactants are expressed by the number of moles per liter of water phase, as indicated by the subscript m. The implication of using $[\,]_m$ instead of $[\,]$ in the above expressions will be given in the Discussion. $[Cl^-]_m$ and $[H_2O]_m$ are equated to 55.5[DPC]/$[H_2O]$ M and 55.5 M, respectively. It is assumed that each DPC molecule provides one Cl^- ion to the micellar water phase and, in addition, that the density of water phase is 1.0 g/mL. K_4 and K_5 are determined to be $(6.0 \pm 1.2) \times 10^{-2} W_0^{-2}$ M^{-2} and $(4.4 \pm 1.5) \times 10^{-1}$ with W_0 = 55.5 M, respectively.[5]

(7) S. S. Zumdahl and R. S. Drago, *J. Am. Chem. Soc.*, **89**, 4319 (1967).
(8) L. H. Pignolet and W. D. Horrocks, Jr., *J. Am. Chem. Soc.*, **90**, 922 (1968).
(9) F. K. Meyer, W. L. Eal, and A. E. Merbach, *Inorg. Chem.*, **18**, 888 (1979).
(10) A. Yamagishi, *Bull. Chem. Soc. Jpn.*, **48**, 2440 (1975).
(11) F. A. Cotton, D. M. L. Goodgame, and M. Goodgame, *J. Am. Chem. Soc.*, **83**, 4690 (1961).

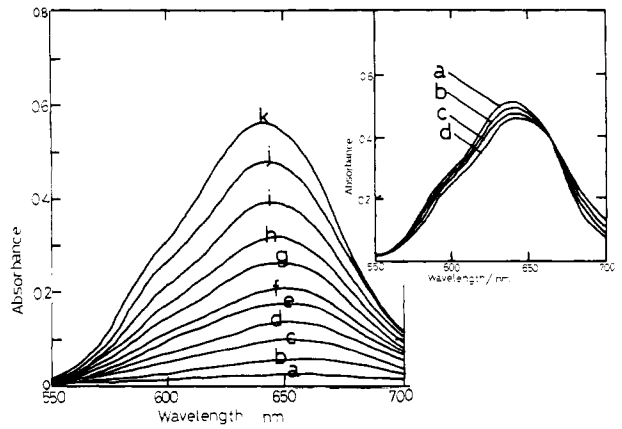

Figure 3. Increase of absorbance in a solution containing $Co(H_2O)_6^{2+}$ in DPC/water/chloroform, when KSCN is added. $[CoCl_2] = 6.6 \times 10^{-4}$ M, [DPC] = 0.15 M, and $[H_2O]$ = 1.2 M. [KSCN] = (a) 0.0020, (b) 0.0028, (c) 0.0040, (d) 0.0050, (e) 0.0059, (f) 0.0060, (g) 0.0079, (h) 0.0088, (i) 0.0100, (j) 0.0114, and (k) 0.0134 M, respectively. The inset shows the absorbance change observed, when DPC is added to a solution containing only $CoCl_2(SCN)_2^{2-}$ and $CoCl_3(SCN)^{2-}$. $[CoCl_2] = 4.4 \times 10^{-4}$ M, [KSCN] = 0.025 M, $[H_2O]$ = 1.48 M, and [DPC] = (a) 0.214, (b) 0.234, (c) 0.259, and (d) 0.287 M, respectively.

At [DPC] = 0.15 M and $[H_2O]$ = 1.2 M, more than 95% of total Co(II) ions are aquated to $Co(H_2O)_6^{2+}$. When KSCN is added to this solution, absorbance increases in the range of 550–740 nm as shown in Figure 3. Considering that the absorbance in this wavelength region is characteristic of the tetrahedral Co(II) complex,[11] the coordination of SCN^- to $Co(H_2O)_6^{2+}$ induces the conversion of octahedral to tetrahedral structure. The absorption peak shifts gradually toward shorter wavelength with increase in KSCN. Thus more than two tetrahedral complexes are involved in complexation processes by SCN^-.

The spectral results are analyzed, assuming that mixed tetrahedral complexes of the type $CoCl_a(SCN)_b(H_2O)_{4-a-b}$ are formed during the above processes. The observed dependence of absorbance on the concentrations of SCN^- and Cl^- is simulated according to eq 6, where A denotes the absorbance, M_0

$$\frac{A}{M_0} = \frac{\sum_a \sum_b \epsilon_{ab} K_{ab} [Cl^-]_m{}^a [SCN^-]_m{}^b}{1 + \sum_a \sum_b K_{ab} [Cl^-]_m{}^a [SCN^-]_m{}^b} \quad (6)$$

is the total analytical concentration of the Co(II) ion, ϵ_{ab} is the molar extinction coefficient of the complex $CoCl_a(SCN)_b(H_2O)_{4-a-b}$, and K_{ab} is the apparent formation constant defined by eq 7. In the above expressions, the intramicellar

$$K_{ab} = \frac{[CoCl_a(SCN)_b(H_2O)_{4-a-b}]_m}{[Co(H_2O)_6^{2+}]_m [Cl^-]_m{}^a [SCN^-]_m{}^b} \quad (7)$$

concentrations of Cl^- and SCN^- are given by $[Cl^-]_m = W_0 - [DPC]/[H_2O]$ and $[SCN^-]_m = W_0[KSCN]/[H_2O]$ with W_0 = 55.5 M, respectively. For the simulation computation, both ϵ_{ab} and K_{ab} are varied over the reasonable ranges which are estimated from the results of the aquation equilibria of $CoCl_4^{2-}$ (eqs 4 and 5). The best values for K_{ab} and ϵ_{ab} are chosen so as to give the minimum of the summation, $\sum_i (A_i^{obsd} - A_i^{calcd})^2$ at a fixed wavelength, where A_i^{obsd} and A_i^{calcd} are the observed and calculated absorbances at the ith value of KSCN concentration, respectively.

In the actual calculations, the possible species among $CoCl_a(SCN)_b(H_2O)_{4-a-b}$ are chosen on the basis of the following facts. (i) At low $[SCN^-]_m$, the absorbances at 580 and 700 nm, A_{580} and A_{700}, increase in proportion to $[SCN^-]_m{}^2$ and $[SCN^-]_m$, respectively. (ii) At the low constant value of

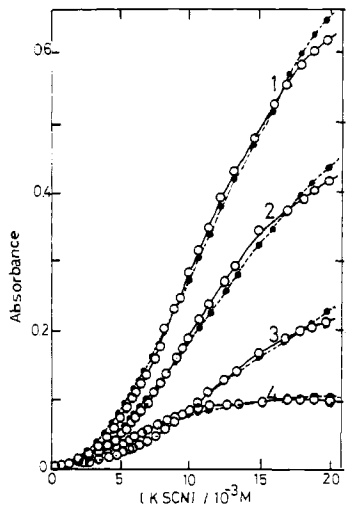

Figure 4. The observed (○) and calculated (●) dependences of absorbance on [KSCN] in the results of Figure 3. The wavelengths are (1) 620, (2) 600, (3) 580, and (4) 700 nm. The calculated curves are based on equilibria 8–10. [KSCN] is extended to 0.020 M.

$[SCN^-]_m$, both A_{580} and A_{700} increase in proportion to $[Cl^-]_m{}^2$. The above facts suggest that $CoCl_2(SCN)_2^{2-}$ and $CoCl_2(SCN)(H_2O)^-$ are responsible for absorptions at 580 and 700 nm, respectively, at least at low $[SCN]_m$. The first simulation is therefore performed to assume equilibria 8 and 9. Equilibria

$$Co(H_2O)_6^{2+} + SCN + 2Cl^- \rightleftharpoons CoCl_2(SCN)(H_2O)^- + 5H_2O \quad K_{21} \quad (8)$$

$$Co(H_2O)_6^{2+} + 2SCN^- + 2Cl^- \rightleftharpoons CoCl_2(SCN)_2^{2-} + 6H_2O \quad K_{22} \quad (9)$$

8 and 9, however, fail in reproducing the experimental results performed at high $[Cl^-]_m$. For improvement of the calculated results, equilibrium 10 is added. Equilibria 8–10 well re-

$$Co(H_2O)_6^{2+} + SCN^- + 3Cl^- \rightleftharpoons CoCl_3(SCN)^{2-} + 6H_2O \quad K_{31} \quad (10)$$

produce the experimental results as exemplified in Figure 4. The simulation using (11) instead of (10) gives A_i^{calcd} deviating

$$Co(H_2O)_6^{2+} + 3SCN^- + Cl^- \rightleftharpoons CoCl(SCN)_3^{2-} + 6H_2O \quad K_{13} \quad (11)$$

from A_i^{obsd} remarkably at high $[SCN^-]_m$. A further trial including equilibrium 12 does not improve the results. Thus

$$Co(H_2O)_6^{2+} + 4SCN^- \rightleftharpoons Co(SCN)_4^{2-} + 6H_2O \quad K_{04} \quad (12)$$

neither $CoCl(SCN)_3^{2-}$ nor $Co(SCN)_4^{2-}$ are formed under the conditions of Figure 3. On the basis of the scheme (8)–(10), the best values for K_{21}, K_{31}, and K_{22} are determined to be $(2 \pm 1) \times 10^{-3}$ M^{-3}, $(8 \pm 4) \times 10^{-4}$ M^{-4}, and $(1.1 \pm 0.5) \times 10^{-2}$ M^{-4}, respectively.

Only two kinds of tetrahedral species, $CoCl_3(SCN)^{2-}$ and $CoCl_2(SCN)_2^{2-}$, are present at the sufficiently high concentration of KSCN. They are in equilibrium (K_{22}/K_{31}; see eq 2). The following facts are consistent with the presence of the above equilibrium. When DPC is added to the solution which is considered to contain only the above two species, the spectrum changes gradually with the isosbestic point at 665 nm (the inset in Figure 3). This corresponds to the displacement of equilibrium 2 to the lefthand side due to the increase of Cl^-. With a plot similar to the inset in Figure 2, the equilibrium constant of (2), K_2, is obtained to be 9 ± 3, which agrees with the ratio of K_{22} to K_{31}, 14 ± 8, within the experimental error.

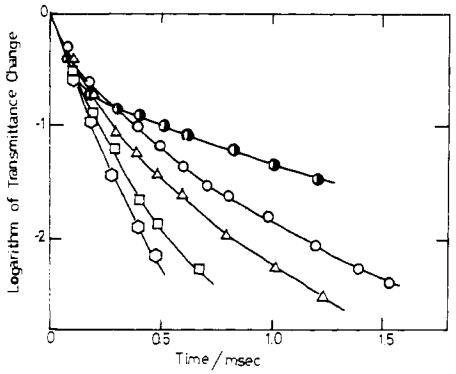

Figure 5. Nonlinear character of the logarithm of transmittance change of a temperature-jump signal vs. time at 650 nm. $[CoCl_2] = 5.5 \times 10^{-4}$ M, $[KSCN] = 5.7 \times 10^{-3}$ M, and [DPC] = 0.41 (◑) and 0.20 M (○). Other plots indicate the effect of water on the relaxational signal at [DPC] = 0.20 M and $[H_2O]$ or $[D_2O] = 0.11$ (△), 0.22 (□), and 0.44 (○) M, respectively.

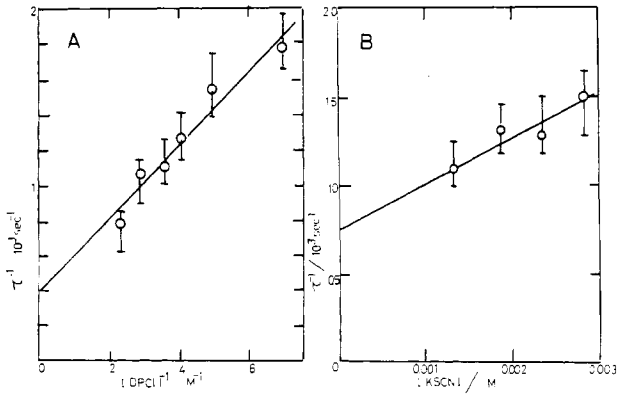

Figure 6. (A) Plot of τ^{-1} against $[DPC]^{-1}$ at $[KSCN] = 5.7 \times 10^{-3}$ M and $[CoCl_2] = 5.5 \times 10^{-4}$ M. The vertical line and circle at each experimental point indicate the upper and lower limit and the average of three to four experimental values, respectively. (B) Plot of τ^{-1} against [KSCN] at [DPC] = 0.20 M and $[CoCl_2] = 5.5 \times 10^{-4}$ M.

Kinetic Results. A chloroform solution of DPC has electrical conductivity high enough to perform Joule-heating temperature-jump measurements.[5] In the absence of any solubilized species, the rapid increase of absorbance is observed at temperature rise in the wavelength below 350 nm. This is ascribed to the interconversion process of DPC aggregates as in eq 13.

$$(DPC)_n + DPC \rightleftharpoons (DPC)_{n+1} \qquad (13)$$

The relaxation rate of (13) is estimated to be higher than 5×10^4 s^{-1} at [DPC] = 0.20–0.50 M.

When electric discharge is performed for a DPC solution containing $CoCl_4^{2-}$ and $CoCl_3(SCN)^{2-}$, the transient change of absorbance is observed at 500–740 nm in the time range of 100 μs. Absorbance stays constant at 685 nm, the isosbestic point of equilibrium 1 (Figure 2). Notably the signal is not a single exponential curve, but it consists of at least two relaxations (Figure 5). As shown in the same figure, the relaxational signal approaches a single exponential curve with the addition of either H_2O or D_2O. There is no isotope effect observed between H_2O and D_2O.

Leaving the detailed discussion on this nonexponential character until the succeeding section, the signal is regarded as having two components; the dependences of the fast and slow relaxation times on [KSCN] and [DPC] are studied. From the results in Figure 6, the following kinetic expression is derived for the slow relaxation:

$$\tau^{-1} = a + b[KSCN]/[DPCl] \qquad (14)$$

with $a = (5.5 \pm 2.0) \times 10^3$ s^{-1} and $b = (3.4 \pm 1.6) \times 10^4$ s^{-1}.

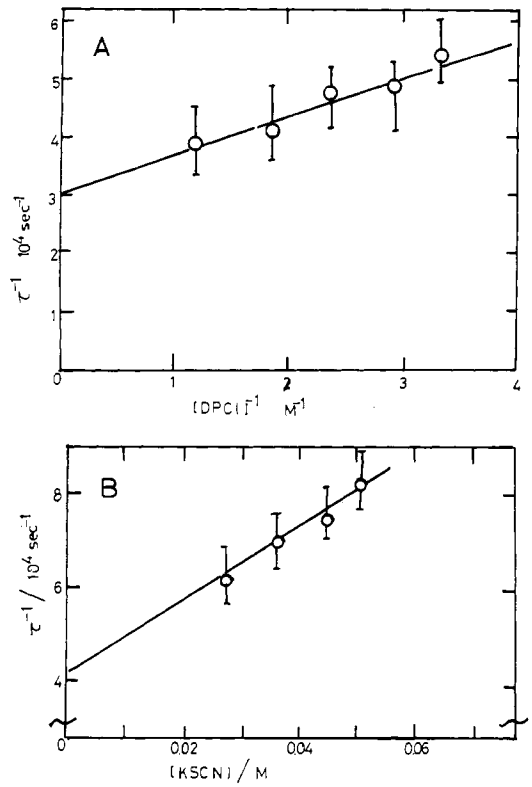

Figure 7. (A) Plot of τ^{-1} against $[DPC]^{-1}$ at [KSCN] = 0.028 M, $[H_2O] = 1.7$ M, and $[CoCl_2] = 1.1 \times 10^{-3}$ M. (B) Plot of τ^{-1} against [KSCN] at [DPC] = 0.20 M, $[H_2O] = 1.7$ M, and $[CoCl_2] = 1.1 \times 10^{-3}$ M.

On the other hand, τ^{-1} for the fast relaxation is almost constant at

$$\tau^{-1} = (2.3 \pm 0.2) \times 10^4 \text{ s}^{-1} \qquad (15)$$

In addition, the amplitude of the first relaxation decreases with the decrease of DPC, 70% ([DPC] = 0.41 M) and 30% ([DPC] = 0.20 M) at [KSCN] = 0.0057 M.

The similar temperature-jump measurements were performed for a DPC/water/chloroform solution containing only $CoCl_2(SCN)_2^{2-}$ and $CoCl_3(SCN)^{2-}$. In this case, the relaxational signal observed in the time range of 100–20 μs is close to a single exponential. The reciprocal of the relaxation time, τ^{-1}, is plotted against $[Cl^-]^{-1}$ and $[SCN^-]$ in Figure 7 at the constant amount of water. In analogy to eq 14, τ^{-1} is expressed by

$$\tau^{-1} = a' + b'[SCN^-]_m/[Cl^-]_m \qquad (16)$$

with $a' = (3.7 \pm 1.0) \times 10^4$ s^{-1} and $b' = (4.0 \pm 1.0) \times 10^5$ s^{-1}, respectively.

Reactions in Water. For comparison, the electronic spectra are measured for an aqueous solution containing $CoCl_2$, NaCl, and NaSCN. The results are shown in Figure 8. The absorption apppears in the wavelength range between 600 and 700 nm, when more than ~0.3 M SCN^- is added. Absorbance at 615 nm increases with the square of SCN concentration. The results indicate that the coordination of SCN^- on $Co(H_2O)_6^{2+}$ induces the tetrahedral–octahedral interconversion to produce a tetrahedral complex of the type $Co(SCN)_2Cl_n(H_2O)_{2-n}$. At [NaCl] = 0.8 M and [NaSCN] = 2.1 M, at most 5% of total Co(II) ions take a tetrahedral structure, on the assumption that the lower limit of the extinction coefficient of $Co(SCN)_2Cl_n(H_2O)_{2-n}$ is 5×10^2.

Discussion

As is reported in the previous paper[3] DPC forms a small aggregate in chloroform above the concentration of 4×10^{-4}

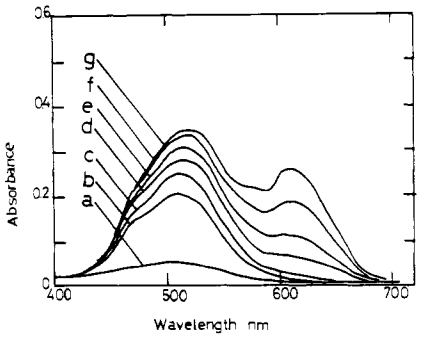

Figure 8. Electronic spectra of Co^{2+} in the aqueous system containing 0.8 M NaCl and a various amount of NaSCN. [NaSCN] = (a) 0, (b) 0.37, (c) 0.68, (d) 1.06, (e) 1.38, (f) 1.78, and (g) 2.10 M and $[CoCl_2] = 9.0 \times 10^{-3}$ M.

M. The average aggregation number, n, increases with the increase of DPC amount according to $n = n_0[DPC]^{0.3}$ with $n_0 = 6.9$.[3] This suggests that the aggregation process is a progressive oligomerization rather than a monomer micelle equilibrium as in eq 13.[12] $CoCl_4^{2-}$ which is highly ionic is believed to be solubilized inside the polar interior of the aggregate. According to eq 13, there exist aggregates of various sizes at a certain value of DPC amount. It is expected therefore that the reactant ions, both $CoCl_4^{2-}$ and SCN^-, may have different reactivities in reaction 1, depending on which size of aggregate they are solubilized in. If this is the case, a relaxational signal is the overlap of several relaxations with different relaxation times as observed in Figure 5. In this respect, the statically obtained equilibrium constant, K_1, which was calculated on the basis of assumptions i–iii is an approximate value averaged over the reactions involving various micellar sizes.

In the presence of water, the aggregation pattern of the surfactant is completely altered.[13] This is, DPC monomers aggregate over the surface of a water droplet with their cationic heads toward the inside of the water phase.[13] Under this aggregation mechanism, the size of the aggregate is dependent only on the ratio of [DPC] to $[H_2O]$.[5,14] If an equilibrium like (1) is established inside an individual micelle, its equilibrium constant is expressed in terms of the intramicellar concentrations as already introduced for K_3 and K_4. In correspondence to this, $CoCl_4^{2-}$ is expected to react with the SCN^- ion at a single rate constant.

The above situations explain why the nonexponential signal observed for reaction 1 approaches an exponential one with the addition of water. Since the amplitude of the fast relaxation decreases with the decrease of [DPC], that relaxation is assigned to the reaction 1 involving large aggregates ($n \gtrsim 4$). On the other hand, the slow relaxation is assigned to reaction 1 involving small aggregates ($n \lesssim 4$). The kinetic expression for the slow relaxation (eq 14) is consistent with the mechanism (17) and (18). With assumption of the

$$CoCl_4^{2-} \rightleftharpoons CoCl_3^- + Cl^- \quad \text{(rapid)} \qquad (17)$$

$$CoCl_3^- + SCN^- \rightleftharpoons CoCl_3(SCN)^{2-} \quad \text{(slow)} \qquad (18)$$

steady-state concentration of the tricoordinate intermediate $CoCl_3^-$, τ^{-1} is given by eq 19. With $[SCN^-] = [KSCN]$ and

$$\tau^{-1} = k_{-18} + (k_{17}k_{18}/k_{-17})[SCN^-]/[Cl^-] \qquad (19)$$

$[Cl^-] = [DPC]$ within the assumptions i–iii, eq 19 coincides with the observed kinetic results ((14)); $k_{-18} = (5.5 \pm 2.0) \times 10^3\ s^{-1}$ and $k_{17}k_{18}/k_{-17} = (3.4 \pm 1.6) \times 10^4\ s^{-1}$. With the ratio of $k_{17}k_{18}/k_{-17}$ taken as k_{-18}, K_1 is calculated to be 6. This value is about 3 times smaller than the equilibrium constant obtained statically. This is because the static K_1 is the average of the equilibrium constants over the aggregates of various sizes.

In contrast to the slow relaxation, τ^{-1} for the fast relaxation is constant for the variations of $[SCN^-]$ and $[Cl^-]$. If the same mechanisms hold for reaction 1 involving large aggregates, the results imply that the first term on the right-hand side in (19) is much larger than the second; $\tau^{-1} = k_{-18} = (2.3 \pm 0.2) \times 10^4\ s^{-1}$. The reason for the larger k_{-18} for large aggregates is not certain.

For reaction 2 in DPC/water/chloroform, the same kinetic expression (16) is obtained. Thus the same scheme (17) and (18) holds for this reaction, leading to the rate constants $k_{-18}' = (3.7 \pm 1.0) \times 10^4\ s^{-1}$ and $k_{17}'k_{18}'/k_{-17}' = (4.0 \pm 1.0) \times 10^5\ s^{-1}$. With taking the ratio of $k_{17}'k_{18}'/k_{-17}'$ taken as k_{-18}', K_2 is calculated to be 11, which agrees with the statically obtained value 9 ± 3 within the experimental error.

The present work revealed that tetrahedral structure of the Co(II) ion is stabilized in reversed micelles. In the absence of water, all Co(II) ions are present as tetrahedral complexes. Even in the presence of water, Co(II) takes the form of the mixed tetrahedral complex $CoCl_a(SCN)_b(H_2O)_{4-a-b}$ (a, b = 1–4) at sufficiently high concentrations of Cl^- or SCN^- ions. Under the conditions in Figure 4, the micellar concentrations of Cl^- and SCN^- ions, defined by $55.5[DPC]/[H_2O]$ M and $55.5[KSCN]/[H_2O]$ M, respectively, are 6.8 and from 0 to 1.0 M, respectively.[15] It is noteworthy that, in bulk water, only 5% of the Co(II) ions take a tetrahedral structure at the comparable amounts of Cl^- and SCN^-. Therefore, the high concentrations of Cl^- or SCN^- ions in micellar water phase are not a sufficient reason to explain the capability of reversed micelle to stabilize the tetrahedral structure.

In order to rationalize the above facts, we postulate that the tetrahedral complexes of Co(II) are not completely solvated inside the micellar water phase of reversed micelles. Instead, these ions are located on the boundary between water phase and surfactant layers, where negative $CoCl_4^{2-}$ complex is attracted toward the positive heads of surfactant molecules. This picture is consistent with the previous ESR studies of metal ions solubilized in the reversed micelles.[3] It was revealed that the tumbling motion of a complex is considerably reduced in comparison with the same metal ions in bulk water. The results were rationalized by assuming that negative metal complexes are fixed over the surfactant layers due to electrostatic attraction. In this boundary region, the attack of water molecules which leads to the conversion of tetrahedral to octahedral structure substantially decreases because of the steric hindrance of bulky surfactant molecules.

Another interesting aspect of the present results is the detection of three-coordinate complex as an intermediate of ligand substitution reactions. This finding is contrasted to the previous NMR studies of the ligand-exchange kinetics of tetrahedral complexes of Co(II) in chloroform. Zumdahl and Drago report that the exchange rate of α-picoline (pic) in the tetrahedral complex $Co(pic)_2Cl_2$ increases in proportion to the α-picoline concentration.[7] This means that the ligand exchange takes place by way of a five-coordinate intermediate, $Co(pic)_3Cl_2$. The similar conclusion is deduced by Pignolet and Horrocks, concerning the ligand exchange of triphenylphosphine derivatives (PPh'_3) in the complex $Co(PPh'_3)_2X_2$, with X = Cl, Br, or I.[8]

There are two possibilities to interpret the present kinetic results. First, a three-coordinate intermediate is preferred to

(12) H. Gutmann and A. S. Kertes, *J. Colloid Interface Sci.*, **51**, 406 (1975).
(13) J. H. Fendler, *Acc. Chem. Res.*, **9**, 153 (1976).
(14) W. G. M. Agterof, J. A. J. Van Zomeren, and A. Vij, *Chem. Phys. Lett.*, **43**, 363 (1976).

(15) The effective concentration of the Cl^- ion which actually participates in the chemical equilibria is previously estimated to be about 25% of [DPC].[5] Thus the effective concentration of Cl^- in Figure 4 is 1.7 M.

a five-coordinate one, when the complex is located in the boundary layer of surfactant molecules. The complex is surrounded by the rigid structures of surfactant molecules so that there is not enough room for the formation of a spacious five-coordinate intermediate. Second, the substituting ligand in the present studies is a negatively charged ion, not the neutral one as in the previous papers. Thus, an entering ligand should overcome the electrostatic repulsion, if an associative five-coordinate intermediate is formed. On the other hand, when a three-coordinate intermediate is formed, the leaving ligand acquires electrostatic energy. At the present stage it is not certain which of the above two possibilities is the more predominant factor for the appearance of the three-coordinate intermediate. We are now intending to perform the kinetic study of ligand substitution of CoX_4^{2-} type complexes in inert solvents.

Acknowledgment. Thanks are due to Professor M. Fujimoto for his encouragement and also due to Mr. U. Nagashima and Mr. M. Takahashi for their assistance in simulating computations.

Registry No. $CoCl_4^{2-}$, 14337-08-7; SCN^-, 302-04-5; $CoCl_3(SCN)^{2-}$, 75673-04-0; $CoCl_2(SCN)_2^{2-}$, 75673-05-1; DPC, 104-74-5; $CHCl_3$, 67-66-3; $CoCl_2$, 7646-79-9; $Co(H_2O)_6^{2+}$, 15276-47-8.

Contribution No. 6238 from Arthur Amos Noyes Laboratories, California Institute of Technology, Pasadena, California 91125

Evaluation of Rate Constants for Redox Self-Exchange Reactions from Electrochemical Measurements with Rotating-Disk Electrodes Coated with Polyelectrolytes

KIYOTAKA SHIGEHARA, NOBORU OYAMA, and FRED C. ANSON*

Received May 22, 1980

A procedure is described for estimating rates of electron self-exchange between multiply charged redox reactants by simple electrochemical measurements with rotating-disk electrodes coated with polyelectrolyte films that spontaneously incorporate the redox reactants by electrostatic attraction. Self-exchange rate constants for the $IrCl_6^{2-/3-}$ and $Fe(CN)_6^{3-/4-}$ couples were evaluated with the new technique to demonstrate its capabilities. The limitations of the method are also described.

Recently we described the versatility of polymer and polyelectrolyte coatings in fashioning electrode surfaces that spontaneously bind large quantities of metal complexes.[1-4] Redox catalysts may be incorporated in such coatings and used to catalyze or mediate electron transfer between the electrode surface and reactants present in the solution.[3] Another possible application of such coated electrodes exists when the species incorporated in the coating is also present in the solution being studied. Under appropriate conditions, the current flowing at such electrodes is limited by the rate of the electron-exchange reaction between the solution-phase reactant and its oxidized (or reduced) counterpart confined within the polyelectrolyte film at the electrode surface. In this paper we describe measurements of such self-exchange rates with two anionic redox couples bound electrostatically to polycationic coatings on graphite electrodes. Related studies have been described recently in which electron-transfer mediators were bound to other kinds of electrode surfaces by nonelectrostatic bonding procedures.[5,6]

Experimental Section

Materials. Pyrolytic graphite electrode were obtained, prepared, and mounted for use as rotating disks as previously described.[1,3] Poly(4-vinylpyridine), PVP, precipitated from methanol–ether, had an average molecular weight of 7.4×10^5. K_2IrCl_6 (RIC) and $K_3Fe(CN)_6$ (Mallinckrodt) were used as received. Supporting electrolytes were prepared from CF_3COOH and CF_3COONa. PVP coatings were prepared as previously described[3] by evaporation of measured aliquots of methanolic solutions of the polymer on the surface of freshly cleaved electrodes. The quantities of the anionic reactants, $IrCl_6^{2-}$ or $Fe(CN)_6^{3-}$, incorporated by protonated PVP films were determined by transferring the electrodes to solutions of pure acidic supporting electrolyte and immediately integrating the current–time curves obtained when the electrode potential was stepped to values well beyond the voltammetric peak potential for reduction of the incorporated reactant. The integration was continued until the current had decreased to background levels. Repetition of the integration procedure showed that only a few percent of the incorporated reactant was lost from the coating during the integration.

Apparatus and Prodecures. Cyclic voltammograms were obtained with PAR Model 173 and 175 instruments (EG & G Instrument Co., Princeton, NJ) and a Houston Instruments X–Y recorder. Rotating-disk current–potential curves were measured with a Pine Instrument Co. (Grove City, PA) electrode rotator and control potentiostat. As noted previously,[3] inclined rather than flat current plateaus were encountered at rotation rates above about 1000 rpm because of inevitable failures in mounting the electrode surfaces exactly perpendicular to their axis of rotation and because the surfaces were not polished. In such cases, limiting currents were taken to be the intersection of lines drawn tangent to the steeply rising portion of the current–potential curve and to the inclined current plateau. Rotating-disk current–potential curves were recorded by scanning the electrode potential at 30 mV s^{-1}. This scan rate produced current peaks in the initial portion of the current–potential curves at low rates of rotation arising from the reduction of the incorporated reactant (e.g., Figure 3). However, as expected, there was no dependence of the steady-state limiting currents on the rate of potential scan. All measurements were conducted at ambient temperature (22 ± 2 °C) in solutions freed of oxygen by bubbling with prepurified argon. Potentials were measured and are reported with respect to a sodium chloride saturated calomel electrode, SSCE.

Results and Discussion

Figure 1A shows a set of cyclic voltammograms recorded successively at a graphite electrode coated with poly(4-vinylpyridine), PVP, in a 2-mM solution of $IrCl_6^{2-}$ at pH 1. The pyridine groups in the polymer coating are protonated at this pH[7] so that the electrode is covered with a polycationic film that spontaneously incorporates multiply charged anions by ion exchange.[2] The incorporation of $IrCl_6^{2-}$ anions by the

(1) Oyama, N.; Anson, F. C. *J. Am. Chem. Soc.* **1979**, *101*, 3450.
(2) Oyama, N.; Anson, F. C. *J. Electrochem. Soc.* **1980**, *127*, 247.
(3) Oyama, N.; Anson, F. C. *Anal. Chem.* **1980**, *52*, 1192.
(4) Oyama, N.; Shimomura, T.; Shigehara, K.; Anson, F. C. *J. Electroanal. Chem.* **1980**, *112*, 271.
(5) Albery, W. J.; Foulds, A. W.; Hall, K. J.; Hillman, A. R. *J. Electrochem. Soc.* **1980**, *127*, 654. Albery, W. J.; Bowen, W. R.; Fisher, F. S.; Foulds, A. W.; Hall, K. S.; Hillman, A. R.; Egdell, R. G.; Orchard, A. F. *J. Electroanal. Chem.* **1980**, *107*, 37.
(6) Lewis, N. S.; Bocarsly, A. B.; Wrighton, M. S. *J. Am. Chem. Soc.*, in press.
(7) Nishikawa, H.; Tsuchida, E. *J. Phys. Chem.* **1975**, *79*, 2072.

0020-1669/81/1320-0518$01.00/0